Nanosized Core-Shell Ni/Au System and its Properties

Ju.A. Zakharov[1,2*], N.K. Yeremenko[2], A.S. Bogomjakov[3], R.P. Kolmykov[1,4], A.N. Yeremenko[2]

[1]Kemerovo State University, Krasnaya st., 6, 650043 Kemerovo, Russia
[2]Institute of coal chemistry and material science SB RAS, Sovietsky Av., 18, 650000, Kemerovo, Russia
[3]The Scientific research institute of the International tomographic center SB RAS, Novosibirsk, Russia
[4]Kemerovo Scientific Centre SB RAS, Sovietsky Av., 18, 650000, Kemerovo, Russia

Article info

Received:
15 October 2014
Received and revised form:
27 November 2014
Accepted:
18 February 2015

Abstract

Core-shell Ni/Au nanoparticles are synthesized by successive reduction of aqueous solutions of nickel sulfate and chloroauric acid by sodium tetrahydroborate. Results of analysis of absorption spectra show that the position of the plasmon absorption peak (507 nm) for Au-shell (1 nm) corresponds to the one for individual gold nanoparticles of the same size. Discussion of the published results about the blocking temperature T_B in the core-shell systems, synthesized by different methods, and obtained results (T_B = 14 ± 0.5 K for nickel core), and HRTEM and elemental analysis results allowed to show that there is linear dependence lgT_B – lgD and T_B – V. It is estimated the average coefficient of magnetic anisotropy $K \approx 4.5 \cdot 10^3$ J/m^3). For Ni-core with special small sizes in the ferromagnetic state there is no magnetization saturation in the field up to 20 kOe. This is the typical behavior for them in the superparamagnetic state also.

1. Introduction

Nanoparticles with the structure of core (a transition metal) – shell (the noble metal) are the most promising area for the practical using in medical hyperthermia (laser or electromagnetic), magnetic resonance imaging and magnetic field-driven medicines transport to the affected area of a body [1-6]. To solve these problems it is required to develop syntheses of chemically pure, sphere-like particles with a narrow size distribution in the nanometer range having a highly magnetic core (electromagnetic hyperthermia from magnetic material). Also they should have 1 nm shell from a noble metal for a core protection and at the same time this shell should be dense enough (to prevent a core oxidation and provide biocompatibility of particles). It is important to examine characteristics and properties of such objects, in particular optical and magnetic ones.

In this work, we will discuss these questions for particles Ni/Au core-shell. Using Au as a shell is in special interest because possibility of its functionalization by different biomolecules [1, 7] and its efficiency of light absorption in the surface plasmons generation.

2. Experimental

Synthesis and results of Ni/Au core-shell particles investigation are described in [8]. As can be seen in [8], the obtained particles have a sphere-like shape, a narrow distribution in sizes (4–8 nm) and Au shell thickness is about 1 nm. As a discontinuity shell surface there is also a layer [NiO + $Ni(OH)_2$] on the Ni-core surface (~ 1 nm), probably it has a form of island formations. There are also signs of very small quantities of bimetallic Au_xNi_y (x >> y) inclusions in the Ni-Au border, and Ni-core contains a small amount of boron impurities.

Vis absorption spectra were recorded using of a PE-5400V spectrophotometer, while superconducting quantum interference device (SQUID) magnetometer (SQUID MPMSXL) was employed to measure magnetic properties of the NPs. Measurements were carried out in fields of up to $2.0 \cdot 10^4$ Oe within the temperature range of 5–300 K.

Determination of blocking temperature of superparamagnetic particle state was realized by measuring the temperature dependence of magnetization (σ) when the samples are cooled in a weak (25 Oe) magnetic field (FC – field cooled regime) and comparing this relationship with the σ – T curve by heat-

* Corresponding author. E-mail: zaharov@kemsu.ru

ing them in the same field after cooling in the field absence (ZFC – zero-field cooled regime).

Temperature and frequency dependence of the real (χ') and imaginary (χ'') parts of the magnetic susceptibility were determined in the frequency range of alternating field 250–1250 Hz from results of experiments in constant magnetic field absence (SQUID magnetometer).

3. Results and Discussion

3.1. Absorption spectra

Ni/Au absorption spectra in the visible spectra range are shown in Fig. 1. There are plasmon resonance bands of Au and Ni/Au against the precursors absorption.

The dependence of position and peaks' width of metal nanoparticles (NPs) plasmon absorption from their sizes, shape, and type of matrix or substrate are complex facts [9], and the combined influence of these factors to the NPs optical absorption characteristics has not been examined enough. Figure 1 shows the plasmon peak of Au-nanoparticles of about 20 nm (i.e. that is close to the size of the synthesized Ni/Au particles).The position of the Au-particles (1–2 nm) absorption peak corresponds to the position of the plasmon peak of Ni/Au particle with gold shell (thickness is ~ 1 nm).

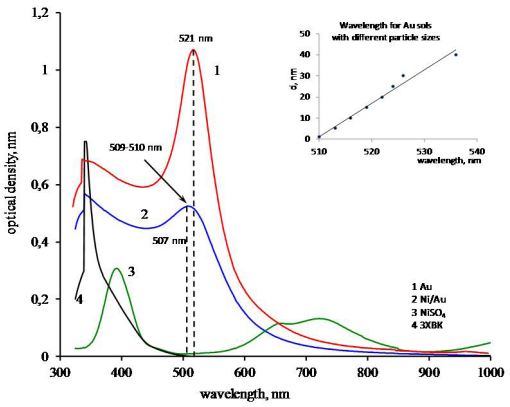

Fig. 1. Optical absorption spectra of precursors, Au colloid with nanoparticles 20–22 nm and Ni/Au core-shell colloid in comparison with position of absorption maximum extrapolated according [10] (the insert) to Au-particles size, corresponding to Au-shell thickness.

It has been shown that gold plasmon peaks formed as nanometer shells of systems (Fe, Co, Ni)/Au shift to the red part of the visible spectra comparatively to plasmon band of spherical Au-nanoparticles [11, 12]. However, size effects (thickness of shell, diameter of matched with them spherical Au-particles) are not taken into account. Our results (identical positions of the shell plasmon peaks and extrapolation value of it for Au particles of the appropriate size) show the need for more detailed study of the matter.

3.2. Magnetic properties

Figure 2 shows the results of determination of magnetization character and the blocking temperature TB (system transition from superparamagnetic state to ferromagnetic one) by classic method of magnetization measuring during cooling in zero and low (25 Oe) magnetic field, and Fig. 5 shows the temperature dependence of the real and imaginary parts of the magnetic susceptibility in the frequency range 250–1250 Hz of magnetic field.

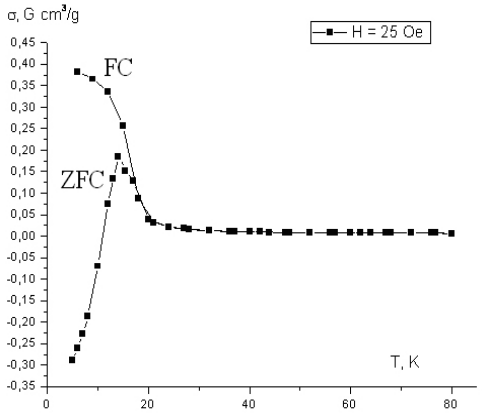

Fig. 2. Temperature dependence of the magnetization of the core-shell Ni/Au nanoparticles, FC and ZFC curves, measured in a 25 Oe applied magnetic field.

From these results T_B (14 ± 0.5 K) is estimated accurately, above this temperature the system Ni/Au is in the superparamagnetic state, and below it the system is in the ferromagnetic one. Ni-cores superparamagnetism is expected from comparison of their estimated in [8] size (4–8 nm) with the known size of a single nickel particles magnetic domain [13].

Existence of a small (up to 2 K on the temperature axis) ZFC and FC curves deflection in the ZFC maximum connects with not monosized Ni-core (Fig. 5). The insignificance of this deviation and agreement of FC and ZFC curves above the T_B region, as well as the temperature dependence of χ'' in different frequencies, indicate a narrow Ni-particle size distribution (that is in agreement with results presented in [8]), and that nanometer Au-shell effectively removes the magnetic (dipolar and transfer) interaction among Ni-particles. From these results we suggest that the effect of possible antiferromagnetic NiO (see. [8]) is not noticeable, because of its very small amounts or possible insular nature of NiO particles. There is no noticeable contribution

of the exchange anisotropy in the Ni-NiO interface, that is supported also by observing symmetry of the magnetization curves in FC mode below T_B.

For single domain superparamagnetic particles with axial magnetocrystalline anisotropy (that, according to [8] and as well as the above mentioned, meets our conditions):

$$T_B = \frac{\Delta E}{k \ln(\tau f_0)} \approx \frac{KV}{25k} \qquad \text{(Eq. 1)}$$

where K – the constant of magnetic anisotropy, k – Boltzmann constant, ΔE – a height of activation barrier, τ – characteristic relaxation time (it corresponds to maximum position of curves in Fig. 5a), f_0 – frequency factor, V – a volume of a single particle.

In [11, 12] measured values of T_B for Ni/Au «core-shell» systems, synthesized by various (others than used by us) chemical methods, Ni-cores have spheroidal nature, narrow size distribution and arguments in favor of Ni-core protection from oxidation by Au-shell are presented. From the Eq. 1 we can deduce (with D_{Ni} is a diameter of Ni-core).

In Figs. 3 and 4 (the plot of $\lg T_B$ versus lgD and the plot of T_B versus (V/25kT) respectively) the two graphs have been constructed using our results, average value of D_{Ni} and Ni-shell thickness given in [11, 12].

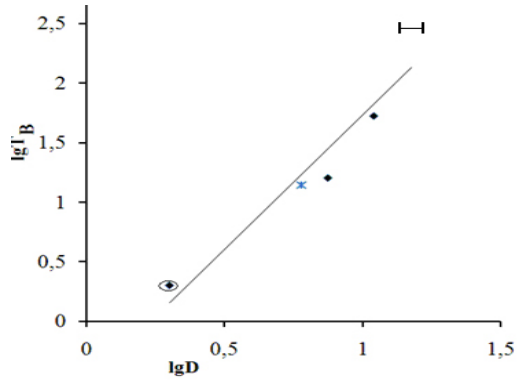

Fig. 3. Dependence (logarithmic coordinates) of the blocking temperature versus lg D (with D = average Ni-core size or Ni-shell thickness).

For the basic part of results realization of Eq. 1 is non-trivial, as we are talking about Ni/Au system synthesized by different methods and using of average values of Ni-core sizes. But there is some variation in sizes according to TEM images and practical agreement of magnetization curves in FC and ZFC regimes, and the dependency of T_B versus KV is not strict one. It is also interesting to notice that the estimated value of anisotropy coefficient $K \approx 4.5 \cdot 10^3$ J/m^3 is almost the same as $K = 5 \cdot 10^3$ J/m^3 reported by Mutler et al. for the massive nickel [15].

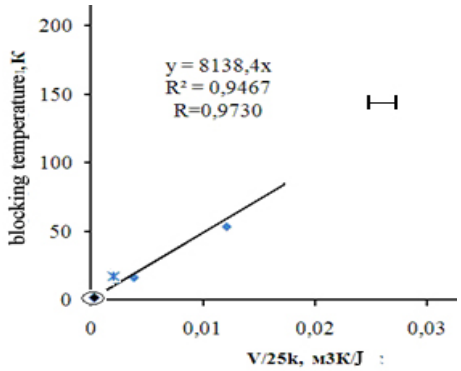

Fig. 4. Dependence of the blocking temperature versus Ni-core volume or Ni-shell for Ni/Au (or Au/Ni) core-shell nanoparticles.

The value $K = 10.48 \cdot 10^3$ J/m^3, which was found from the equation $K = \log(\tau f_0)(kT/V)$ in [11], is more than we found, it is connected with using in [11] of rough approximations $\tau = 30$ sec (measurement time), usually for superparamagnets $f_0 = 10^9 - 10^{11}$s^{-1} using a logarithm to the base 10.

The significant error of results in Figs. 3 and 4 is due to the considerable variation of Ni-cores in [12].

Analysis of temperature and frequency dependence of the maxima position in curves $\chi'(T)$ for measurements in the constant magnetic field absence shows satisfactory realization of Eq. 1 in its strict part (inset in Fig. 5). This corresponds to the model of thermally activated relaxation of superparamagnetic with nanoparticles magnetocrystalline anisotropy, while overcoming the activation barrier ΔE, and it allows to evaluate the approximation from $\tau^{-1} = f_0 \exp(-\Delta E/kTB)$ (from Eq. 1) frequency factor ($f_0 \approx 10^{13} - 10^{14}$ s^{-1}) and $\Delta E/K$ (≈ 840 K).

The estimated values are higher than typical ones for superparamagnets (see, e.g. [14]). In this regard it should be noted that our preliminary evaluation due to the very limited number of measured values for $(\chi', \chi'') = f(\nu, T)$ and a narrow frequencies range. The latter is associated with the ability of used SQUID-magnetometer.

The magnetization curves of Ni/Au and the magnetization dependence from temperature at 20 kOe are shown in Figs. 6 and 7, respectively. In the ferromagnetic state coercivity is 750 Oe at 5 K and decreases with increasing temperature (up to 400 Oe at 12 K). Magnetization does not reach saturation in the field at 20 kOe, that may be related to the presence (see [8]) of small NiO amounts, which has a strong magnetic anisotropy, and (or) spin-frozen states near the surface of nanosized Ni-core. There is no observed saturation in relatively high magnetic fields for nanostructured Ni particles with Ni-core 4-8 nm according to [8] and for crystallites Ni/Au with similar core sizes (5–10 nm) [11, 16], but a such situation is not observed for Ni/Au with bigger Ni-cores [12].

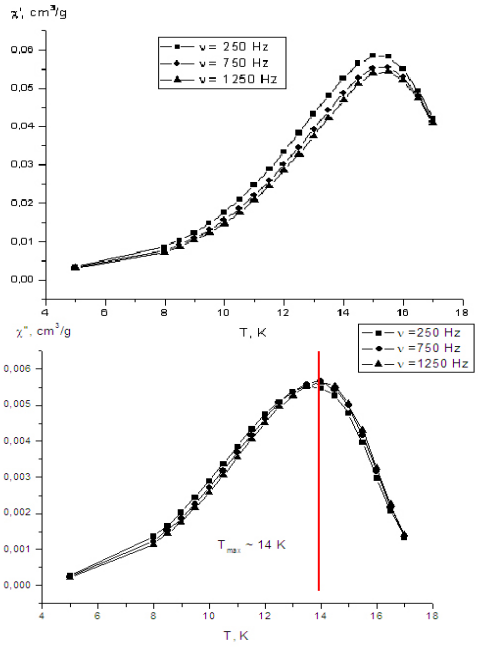

Fig. 5. Temperature dependence of (a) real (χ') and (b) imaginary (χ'') parts of magnetic susceptibility for Ni/Au core-shell nanoparticles.

Normalized by results of elemental analysis and TEM [8, 11, 12] saturation magnetization σn is 65–67 emu/g for Ni/Au with big Ni-cores [12], 62 emu/g for a massive Ni at 5 K; and in the field 20 kOe magnetization is 46–48 emu/g for Ni/Au from this work and 66–68 emu/g for nanostructured nickel [16]. These results illustrate a little influence of synthesis methods and particle morphology to σ_n in ferromagnetic state, and at the same time σ_n reducing for Ni/Au with cores, which are less than 10 nm, (according our results and [11], where σ_n decreases to 9 emu/g, despite the fact that the size of Ni-cores (5–10 nm) is slightly bigger than in the particles synthesized by us). σ reducing with decreasing of metal nanoparticles size is a common phenomenon [13]; for Ni/Au system the above mentioned features of Ni-cores magnetic properties should be taken into account.

When Ni-core is in the superparamagnetic state ($T > T_B$), as it should be, it does not have a coercivity (Fig. 6, and also [11, 12]).

Simultaneously magnetization of Ni-cores is specifically. For Ni/Au systems with small Ni-cores (≤ 10 nm, see. Figs. 6 and 7 and [11]) there is a sharp (compared to the ferromagnetic state) decreasing of the magnetization and there is no saturation in fields up to 20 kOe.

As core size reducing this effect is more obvious. So, for our Ni/Au particles with a core of about 6 nm normalized to the mass of nickel magnetization is only about 1 emu/g at 300 K in the field of 20 kOe, and the dependence $\sigma - H$ is linear one (Fig. 6). The magnetization decreases sharply with increasing temperature from 5 to 50 K (Fig. 7). For Au/Ni particles with 2 nm Ni-shell and $T_B < 2K$ in the field of 5 kOe (limit value is shown in [14]) magnetization curve is also linear one, and the magnetization is about 0.9 emu/g. For Au/Ni with a slightly larger core (5–10 nm) the curve σ-H is saturated at ~ 5kOe, and σ_n is ~ 0.7 emu/g [11]. In contrast, for Ni/Au with bigger Ni-cores (14–15 nm) normalized value of σn is ~ 45–47 emu/g at 300 K, that is only slightly smaller than σ_n ~ 66 emu/g at 5 K, and magnetization was saturated when the applied magnetic field reached ~ 5 kOe [12].

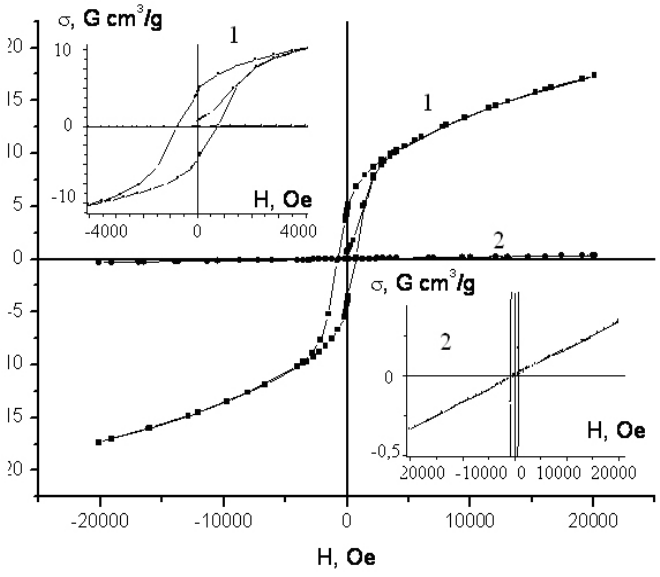

Fig. 6. Ni/Au magnetization curves at 5 K (1) and 300 K (2).

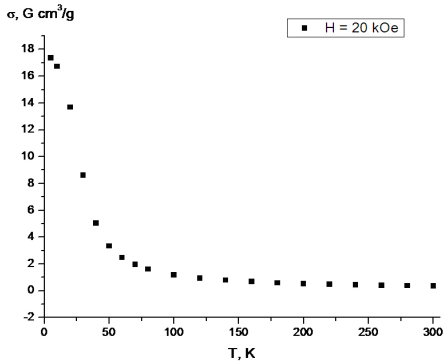

Fig. 7. Temperature dependence of the magnetization of the core-shell Ni/Au nanoparticles measured in a 20 kOe applied magnetic field.

For nanoscale core-shell systems with a core from ferromagnetic metal information about the magnetic properties features is limited to the above mentioned. Further studies are needed for clarification of its nature, including the effect of Ni-core sizes, shell thickness, and the possible role of oxidation processes in the cores, and in the whole, generality of the observed effects for the systems «core (metal ferro-, superparamagnetic state) – shell (the noble metal)». Influence of the Ni-core sizes is registered qualitatively and it shows that this effect is most likely related to the formation of "frozen" spin subsystem at the Ni-Au interface. It is also necessary to clarify the influence of nanoscale inclusions of nickel oxidation products and to specify formation and the role of mixed Ni-Au nanophases [8]. To the present time thin Au-shell (3–4 nm) has been synthesized, and it defends Ni-core from oxidation. The investigation of magnetic properties of such a system has been started.

4. Conclusions

The absorption spectrum of the colloid-forming core-shell Ni/Au nanoparticles, with nanometer Au-shell, exhibits an absorption band with a maximum at 507 nm, that corresponds to the band position of the single Au nanoparticles of the same size.

The position of the peak at 507 nm indicates atypical blue shifting for such systems. The red shift in wavelength of gold surface plasmon can be usually observed in other bimetallic systems.

Analysis of published information and our results allowed showing that for the main part of the results the linear dependence lgT_B versus lgD and T_B versus V (the average volume of the cores) is realized. It is possible to estimate the average value of the magnetic anisotropy $K \approx 4.5 \cdot 10^3$ J/m^3, a value $5 \cdot 10^3$ J/m^3 was reported for bulk metal.

When Ni/Au nanoparticles with a smaller-sized Ni core (less than 10 nm in a diameter) are in the ferromagnetic state (temperature is below than T_B) the magnetization was not saturated even when the applied field reached 20 kOe. This is typical for it in the superparamagnetic state also. When Ni/Au nanoparticles transit from the ferromagnetic state to the superparamagnetic one, a sharp (from ≈ 50 emu/g to ≈ 1 emu/g) decreasing of the magnetization, especially significant one in the field of 50–60 K, can be observed. The core-shell Ni/Au nanoparticles with inert gold coatings presented here show a great promise as nickel-based nanoparticles.

Acknowledgments

The authors acknowledge the financial support by the Russian Ministry of Education and Science (project 2014/64), using shared equipment of the Kemerovo Science Centre of SB RAS.

References

[1]. In Osama O. Avadelkarim (ed.), Chunli Bay (ed.), S.P. Kapitsca (ed.), E.E. Demidova (ed.). Nanoscience and nanotechnology. Encyclopedia of Life Support Systems. Unesco: eolss : id magistr press, Moscow, 2011, p.1000.

[2]. Capek, in Osama O. Avadelkarim (ed.), Chunli Bay (ed.), S.P. Kapitsca (ed.), E.E. Demidova (ed.). Nanosensors – sensors on the basis of metal and compound nanoparticles and nanomaterials and nanotechnology. Encyclopedia of Life Support Systems. unesco: eolss: id magistr press, Moscow, 2011, p.858.

[3]. D.S. Wang, J.B. He, N. Rosenzweig, Z. Rosenzweig; Nano Lett. 4 (2004) 409–413.

[4]. J. Cheon and J.-H. Lee, Acc. Chem. Res. 41 (2008) 1630–1640.

[5]. J. Gao, H. Gu and B. Xu, Acc. Chem. Res. 42 (2009) 1097–1107.

[6]. J.-W. Jun, Y.-W. Seo and J. Cheon; Acc. Chem. Res. 41 (2008) 179–189.

[7]. M.-C. Daniel, D. Astruc, Chem. Rev. 104 (2004) 293–346.

[8]. Ju. Zakharov, N. Yeremenko, V. Dodonov, V. Pugachev, D. Russakov, N. Ivanova, A Yeremenko, I. Obraztsova, Eurasian Chemico-Technological Journal, accepted for publication.

[9]. S. Cho, J. Idrobo, J. Olamit, Chem. Mater. 17 (2005) 3181–3186.

[10]. V. Ignatov, (ed.), L. Dikman, V. Bogatirev, S. Schegolev, N. Khlebscov; Nauka, Moscow, 2008, p.46.

[11]. D. Chen, J. Li, Ch. Shi, X. Du, N. Zhao, J. Sheng and S. Liu, Chem. Mater. 19 (2007) 3399–3405.

[12]. H. She, Yu. Chen; J. Mater. Chem. 22 (2012) 2757–2765.
[13]. D. Ryzhonkov, V. Levina, E. Dzidziguri; Nanomaterials. Binom, Moscow, 2008. – p.365.
[14]. J. Bondi, R. Mistra, X. Ke, I. Sines, and R. Schaak; Chem. Mater., 22 (2010) 3988–3994.
[15]. R. Mutler, A. Aydinuraz, J. Magn. Mater. 68 (1987) 328–330.
[16]. R.P. Kolmykov. Synthesis and properties investigation of nickel and cobalt nanopowders and their system // Diss. Ph.D. – Kemerovo State University. 2011. – p.21.